

New gap-filling and partitioning technique for H_2O eddy fluxes measured over forests

Minseok Kang¹, Joon Kim^{1,2,3,4}, Bindu Malla Thakuri², Junghwa Chun⁵, Chunho Cho⁶

¹National Center for AgroMeteorology, Seoul, 08826, South Korea

⁵²Program in Rural Systems Engineering, Department of Landscape Architecture & Rural Systems Engineering, Seoul National University, Seoul, 08826, South Korea

³Interdisciplinary Program in Agricultural & Forest Meteorology, Seoul National University, Seoul, 08826, South Korea

⁴Institute of Green Bio Science and Technology, Seoul National University Pyeongchang Campus, Pyeongchang, 25354, South Korea

¹⁰⁵Department of Forest Conservation, National Institute of Forest Science, Seoul, 02455, South Korea

⁶National Institute of Meteorological Research, Seogwipo, 63568, South Korea

Correspondence to: Minseok Kang (ms-kang@ncam.kr)

Abstract. The continuous measurement of H_2O fluxes using the eddy covariance (EC) technique is still challenging for forests because of large amounts of wet canopy evaporation (E_{WC}), which occur during and following rain events when the

¹⁵ EC systems rarely work correctly. We propose a new gap-filling and partitioning technique for the H_2O fluxes: a model-stats hybrid method (MSH). It enables the recovery of the missing E_{WC} in the traditional gap-filling method and the partitioning of the evapotranspiration (ET) into transpiration and (wet canopy) evaporation. We tested and validated the new method using the datasets from two flux towers, which are located at forests in hilly and complex terrains. The MSH reasonably recovered the missing E_{WC} of $16 \sim 41 \text{ mm year}^{-1}$ and separated it from the ET (14 ~ 23% of the annual ET). Additionally, we illustrated ²⁰ certain advantages of the proposed technique, which enables us to understand better how ET responses to environmental changes and how the water cycle is connected to the carbon cycle in a forest ecosystem.

1 Introduction

Forest ecosystems share three properties that are significant in their interactions with the atmosphere. They are extensive, ²⁵ dense and tall, and thus produce sizable aerodynamic roughness and canopy storage for rainfall interception/evaporation (e.g., Shuttleworth, 1989). Since most of the flat terrains are used as agricultural lands and towns (or cities), substantial areas of forest exist in mountainous terrains where the fundamental assumptions of eddy covariance (EC) measurement (flat and homogeneous site, e.g., Baldocchi et al., 1988) are violated. These facts hinder the use of the EC method from assessing the net ecosystem exchanges (NEE) of H_2O and CO_2 in forests.

³⁰ Considering that EC measures compound ‘net’ fluxes and its gaps are unavoidable, we commonly take great care for flux gap-filling and partitioning. Basically, the gap-filling and partitioning are a kind of interpolation and extrapolation based on

that EC measurement has high temporal resolution and the bio-meteorological processes is a (repetitive) cycle (“redundancy” of data) (Papale et al., 2012). Generally, they consist of the following procedure: (1) setting a target flux (e.g., $\text{CO}_2/\text{H}_2\text{O}/\text{CH}_4$ fluxes, ecosystem respiration), (2) selecting drivers which control the target flux, (3) identifying relationships between the (appropriate) target flux (which can represent true NEE) and the drivers, and (4) interpolating and extrapolating the relationships during a certain period when the relationship is maintained (e.g., Papale et al., 2012; Reichstein et al., 2012). In this context, the gap-filling and partitioning (including nighttime CO_2 flux correction) are coterminous with each other. The related scientific issue is determining/selecting the number and type of drivers, and the method and the time window size to identify the relationship. It depends on data availability, temporal scale of the process, and ecosystem state change. Those processes require extra care for the measurement in complex mountainous terrain(e.g., van Gorsel et al., 2009; Kang et al., 2017).

Wet canopy evaporation (E_{WC}) is an evaporation of the intercepted water by the vegetation canopy during and following rain events, which may consist of a significant portion of evapotranspiration (ET). Over forests, it is hard to measure the E_{WC} primarily due to the malfunction of an open-path EC system with rainfall. Although a closed-path system with an intake tube enables the E_{WC} measurement in the rain, the attenuation of the turbulent flow inside the tube acts as a low-pass filtering, which results in a significant underestimation of the E_{WC} . Furthermore, the attenuation domain expands with an increasing relative humidity (RH) from high frequency to medium frequency (e.g., Ibrom et al., 2007; Fratini et al., 2012). The closed-path EC system with the heated tube may be the most appropriate for measuring ET in the rain (e.g., Goodrich et al., 2016). The missing (or low quality) data can be gap-filled using general gap-filling methods such as the marginal distribution sampling and artificial neural network (e.g., Reichstein et al., 2005; Papale and Valentini 2003). However, Kang et al. (2012) showed that, without a proper consideration of the E_{WC} , such gap-filled ET data under the wet canopy conditions are underestimated because the data used in such gap-filling are mostly collected dry or partially wet canopy condition when the EC systems work properly. The authors proposed an improved gap-filling method that is coupled with a simple canopy (water) interception model.

The ET represents a combination of the E_{WC} , transpiration (T), and soil evaporation (E_S), which are controlled by different mechanisms and processes. Therefore, the partitioning of ET into the E_{WC} , T , and E_S is required to understand how ET is regulated by environmental changes and the how water cycle is connected to the carbon cycle in a forest ecosystem. For these reasons, there have been many previous studies that partition ET using other supplementary measurements or empirical/process models (e.g., Wilson et al., 2001; Yepez et al., 2003; Daikoku et al., 2008; Stoy et al., 2006; Hu et al., 2009; Kang et al., 2009b). Despite the many previous studies on ET partitioning, most of them have focused on the partitioning of ET into the E_S (or direct evaporation, i.e., a sum of E_S and E_{WC}) and T . In the case of forest ecosystems with a dense canopy under a monsoon climate (e.g., East Asia, South Asia), the E_{WC} can play a greater role than the E_S . In this context, it is necessary to pay attention to the method described by Kang et al. (2012), which not only allows the proper estimation and gap-filling of the missing evaporation data under wet canopy conditions but also enables the partitioning of ET into the E_{WC} and T appropriately after certain modifications.

In this study, we propose a new gap-filling and partitioning technique for the H_2O fluxes measured over forests in complex mountainous terrain. First, we introduce a model-stats hybrid method, which can not only recover the missing E_{WC} in the general gap-filling method but also separate it from ET. Then, we tested and validated these new methods using the datasets from the two flux towers, which are located in forests with hilly and complex terrains. Additionally, we illustrated certain 5 advantages of the new technique.

2 Materials and Methods

2.1 Study sites

In the Gwangneung National Arboretum, there are two eddy covariance flux towers: the Gwangneung deciduous forest located at the top of a hill (GDK; $37^{\circ} 45' 25''$ N, $127^{\circ} 09' 12''$ E) and the Gwangneung coniferous forest located at the 10 bottom (GCK; $37^{\circ} 44' 54''$ N, $127^{\circ} 09' 45''$ E). Gwangneung has been protected to minimize human disturbance over the last 500 years. Both sites are located on complex, hilly catchment with a mean slope of $10 - 20^{\circ}$. The two towers are ~ 1.2 km apart, and the mean slope between them is $\sim 6.2^{\circ}$ (Moon et al., 2005). The east/west slopes are gentle, whereas the 15 north/south slopes are steep in the catchment. The mountain-valley circulation is dominant wind regime in the sites (Hong et al., 2005; Yuan et al., 2007). Meteorological records from an automatic weather station ~ 1.6 km northeast of the tower for 1997-2016 show that annual mean air temperature is $10.1 \pm 0.6^{\circ}\text{C}$ and the mean precipitation is $1,472 \pm 352$ mm (National Climate Data Service System, <http://sts.kma.go.kr/>). At the GDK site, the vegetation is dominated by an old natural forest of *Quercus* sp. and *Carpinus* sp. (80 – 200 years old) with a mean canopy height of ~ 18 m and a maximum leaf area index (LAI) of $\sim 6 \text{ m}^2 \text{ m}^{-2}$ in June. Compared to the GDK site, the GCK site is in a lower area and is a flat, plantation forest with the dominant species of *Abies holophylla* (approximately 80 years old) with a mean canopy height of ~ 23 m and a maximum 20 LAI of $\sim 8 \text{ m}^2 \text{ m}^{-2}$ in June. Further descriptions of the sites can be found in Kim et al. (2006) and Kang et al. (2017).

2.2 Measurements and data processing

The H_2O and CO_2 fluxes have been measured since 2006 and 2007 at the GDK site and GCK site, respectively. At both sites, the EC system was used to measure the fluxes from a 40 m tower. The wind speed and temperature were measured with a three-dimensional sonic anemometer (Model CSAT3, Campbell Scientific Inc., Logan, Utah, USA), while the H_2O and CO_2 25 concentrations were measured with an open-path infrared gas analyzer (IRGA; Model LI-7500, LI-COR Inc., Lincoln, Nebraska, USA) at both sites. Half-hourly ECs and the associated statistics were calculated online from the 10 Hz raw data and stored in dataloggers (Model CR5000, Campbell Scientific Inc.). Other measurements such as net radiation, air temperature, humidity, and precipitation were sampled every second, averaged over 30 minutes, and logged in the dataloggers (Model CR3000 for the GDK site and CR1000 for the GCK site, Campbell Scientific Inc.). More information 30 regarding the EC and meteorological measurements can be found in Kwon et al. (2009), and Kang et al. (2009a).

The multi-level profile systems were installed to measure the vertical profiles of the CO₂ and H₂O concentrations at both sites and to estimate the storage flux using a closed-path IRGA (Model: LI-6262, LI-COR Inc.). The measurement heights were 0.1, 1, 4, 8 (base of the crown), 12 (middle of the crown), 18 (the canopy top), 30, and 40 m for the GDK site and 0.1, 1, 4, 12 (base of the crown), 20 (middle of the crown), 23 (the canopy top), 30, and 40 m for the GCK site. More information 5 regarding the multi-level profile system can be found in Hong et al. (2008) and Yoo et al. (2009).

To improve the data quality, the collected data were examined by the quality control procedure based on the KoFlux data processing protocol (Hong et al., 2009; Kang et al., 2014). This procedure includes a sector-wise planar fit rotation (PFR; Wilczak et al., 2001; Yuan et al., 2007; Yuan et al., 2011), the WPL (Webb-Pearman-Leuning) correction (Webb et al., 10 1980), a storage term calculation (Papale et al., 2006), spike detection (Papale et al., 2006), gap-filling (marginal distribution sampling method; Reichstein et al., 2005), and nighttime CO₂ flux correction (van Gorsel et al., 2009; Kang et al., 2016). The details of the gap-filling and partitioning methods are described in the next chapters.

2.3 Gap-filling and partitioning methods for the H₂O flux

2.3.1 Marginal distribution sampling (MDS) method

The missing H₂O flux (i.e., evapotranspiration, ET) data were gap-filled using the marginal distribution sampling (MDS) 15 method (Reichstein et al., 2005; Hong et al., 2009). This method calculates a median of ET under similar meteorological conditions within a time window of 14 days and replaces the missing values with the median. The intervals of the similar meteorological conditions were 50 W m⁻² for the downward shortwave radiation (R_{sdn}), 2.5°C for the air temperature (T_a), and 5.0 hPa for the vapor pressure deficit (VPD). If similar meteorological conditions were unavailable within the time 20 window, its interval increased in increments of 7 days before and after the missing data point (i.e., 14 days of window size) until it reached 56 days (i.e., before and after 7 days → 14 days → 21 days → 28 days). When the missing ET values could not be filled in a time window less than 56 days, R_{sdn} was exclusively used following the same approach (i.e., calculating a median of ET under similar R_{sdn} conditions within a time window). This gap-filling method is used for not only the H₂O flux but also the sensible heat and daytime CO₂ fluxes.

2.3.2 Modeling of wet canopy evaporation

25 For estimating the wet canopy evaporation (E_{WC}), a simplified version of the Rutter sparse model (Valente et al., 1997) included in the VIC LSM (Variable Infiltration Capacity Land Surface Model, Liang et al., 1994) was used in the KoFlux data processing program. The E_{WC} is estimated as follows:

$$E_{WC_Mod} = \sigma_f E_p \left(\frac{W_c}{S} \right)^n \left(\frac{r_a}{r_a + r_0} \right) \quad (1)$$

where E_{WC_Mod} is the modeled E_{WC} , σ_f is the vegetation fraction (i.e., 1-gap fraction); and E_p is the potential evaporation

$$E_p = \frac{\varepsilon A + \rho c_p \cdot VPD \cdot g_a / \gamma}{\lambda(\varepsilon + 1)}$$

where ε is the dimensionless ratio of the slope of the saturation vapor pressure curve to

the psychrometric constant γ , A is the available energy, ρ is the density of air, c_p is the specific heat of air, g_a is the aerodynamic conductance ($= 1 / r_a$), λ is the latent heat of vaporization); r_a is the aerodynamic resistance to heat and water

5 vapor transport; S is the canopy storage capacity; and r_0 is the architectural resistance. The term, $(r_a / (r_a + r_0))$, is added to consider the variation of the gradient of specific humidity between the leaves and the overlying air in the canopy layer. W_c is the intercepted canopy water, and the exponent n is an empirical coefficient.

W_c is estimated as:

$$\frac{\partial W_c}{\partial t} = \sigma_f P - D - E_{WC_Mod} \quad (2)$$

10 where P is the input total rainfall and D is the drip. When $W_c > 0$, the canopies are wet. When $W_c > S$, the drip starts ($D > 0$). There are many inputs (i.e., E_p and P) and parameters (i.e., σ_f , S , n , r_a , and r_0) for estimating the E_{WC} and W_c . E_p , P , and r_a ($= r_{am} + r_b$ where r_{am} and r_b are the aerodynamic resistance of momentum transfer and the excess resistance; $r_{am} = \bar{U} / u_*$

where \bar{U} is the wind speed, u^* is the friction velocity; $r_b \approx \frac{4.63}{u_*}$; Thom, 1972; Kim and Verma, 1990; Kang et al., 2009a)

can be obtained/estimated from the flux tower measurement. The parameters can be divided into constant parameters (i.e., n and r_0) and seasonally varied parameters (i.e., σ_f and S). The default values (before optimization) of n and r_0 are 2/3 and 2 s

15 m^{-1} , respectively. σ_f ($= 1 - \text{gap fraction}$) and S are functions of LAI (leaf area index): (1) the gap fraction is estimated by $\exp(-k \times \text{LAI})$, where k varies from 0.3 to 1.5, depending on the species and canopy structure (Jones, 2013, $k = 0.75$ and 0.485 for the GDK and GCK, respectively; (2) S is estimated by $K_L \times \text{LAI}$, where K_L varies from 0.1 to 0.3 (default value of $K_L = 0.2$, see Appendix A for more details). σ_f and LAI can be obtained from a plant canopy analyzer or digital photography

20 (e.g., Macfarlane et al., 2007, Hwang et al., 2016). If actual measurement is not available, MODIS (moderate-resolution imaging spectroradiometer) LAI can be used alternatively. In this study, σ_f (actually k) and LAI were estimated using a plant canopy analyzer (Model LAI-2000; Li-Cor Inc.).

The generalization of the model can be augmented by providing the parameter optimization procedure using available flux data under wet canopy condition. We argue that this is better than the validation using other datasets because the parameters

25 may be site-specific (i.e., more validation does not fully guarantee the proposed model works properly everywhere). After optimizing the parameters (i.e., K_L , n , and r_0), the parameters slightly changed from the default values (see Appendix B for more details). Since the model results from before and after the parameter optimization were not statistically different in the error assessment, we still used the default values in a conservative way.

This method only considers the E_{WC} from the canopy by neglecting the E_{WC} from the trunk and stem. Besides, the interception of snow is not considered because the small amount of intercepted snowfall evaporates when the eddy covariance systems function improperly, and its melting and sublimation processes are much more complex than intercepted rainfall. To distinguish snowfall from total precipitation, the empirical discriminants in Matsuo et al. (1981) were used. This 5 method uses air temperature and humidity near the ground surface to separate snow from rainfall because when it snows, air is not saturated and the near ground air temperature is lower than that under rainy condition. The result from this method should be scrutinized by comparing it with other precipitation data, which are measured at a weather station near the site.

2.3.3 Gap-filling and partitioning technique for evapotranspiration: model-stats hybrid method

The currently used MDS is expected to under- and over-estimate ET under wet and dry canopy conditions, respectively due 10 to the gap-filling without the consideration of canopy wetness (because the evaporative fraction is proportional to canopy wetness). Therefore, the gap-filling technique for ET proposed by Kang et al. (2012) was used: (1) to identify the canopy wetness, the intercepted canopy water (W_c , see Eq. 1) was calculated using the simplified Rutter sparse model; (2) all the missing gaps were filled by the MDS using the data under dry canopy conditions only (i.e., when $W_c = 0$), which corresponds to the ET under dry canopy condition (ET_{dry}); (3) under wet canopy conditions (i.e., when $W_c > 0$), the gap-filled data were 15 replaced with the sum of the E_{WC} estimated by the simplified Rutter sparse model (i.e., E_{WC_Mod}) and the ET_{dry} multiplied by $1-(W_c/S)^n$ (i.e., the contribution from transpiration) (see Eqs. 1 and 2).

Such a gap-filled ET was partitioned into the transpiration (T or ET from the dry canopy, which approaches the actual transpiration under a dense and closed canopy condition) and E_{WC} as follows. In case of that the data was missing, the T was estimated as $(1-(W_c/S)^n) ET_{dry}$, while the E_{WC} was estimated as E_{WC_Mod} . In case of that the data was not missing (i.e., ET_{Obs}), 20 the partitioning procedure divided into two parts. If the signs of ET_{Obs} , ET_{dry} , and E_{WC_Mod} were the same, the T was estimated by multiplying ET_{Obs} and the ratios of $(1-(W_c/S)^n) ET_{dry}$ to the sum of $(1-(W_c/S)^n) ET_{dry}$ and E_{WC_Mod} (i.e., the estimated transpired-fraction of ET), while the E_{WC} was estimated by multiplying ET_{Obs} and the ratios of E_{WC_Mod} to the sum of $(1-(W_c/S)^n) ET_{dry}$ and E_{WC_Mod} (i.e., the estimated evaporated-fraction of ET). If the signs of ET_{Obs} , ET_{dry} , and E_{WC_Mod} 25 were not the same, the T were estimated by $(1-(W_c/S)^n) ET_{dry}$, while the E_{WC} was estimated by subtracting $(1-(W_c/S)^n) ET_{dry}$ (i.e., the estimated T) from ET_{Obs} . The procedure regarding the MSH is described in Fig. 1.

[Figure 1 here]

3 Results

3.1 Validation of the MSH

First, we evaluated the latent heat flux under (mostly) wet canopy conditions (λET_{WC} , i.e., λET when $W_c/S > 2/3$) from the model-stats hybrid (MSH) method (λET_{WC_MSH}) against the observed λET_{WC} (λET_{WC_Obs}) at both sites from 2008 to 2010

5 (Fig. 2). Since the λET_{WC} occurs in during and following rain events, open-path EC system can measure the λET_{WC} when the instrument dries out faster than the canopy. Most of the points are near a one-to-one line. The data scattered away from the one-to-one line are characterized by large aerodynamic conductance (e.g., $>100 \text{ mm s}^{-1}$) and/or large VPD (e.g., $>10 \text{ hPa}$).

[Figure 2 here]

10

Table 1 shows the statistical parameters for the error assessment (i.e., MBE, MAE, RMSE, d , slope, and r^2 ; see Appendix D for more details about the error assessment). The slopes from the linear regression analysis are 0.97 ± 0.15 and 0.89 ± 0.07 with 0.69 ± 0.06 and 0.81 ± 0.02 of r^2 for the GDK and GCK sites, respectively. The d values for the sites were close to 1 (0.91 \pm 0.01 for the GDK and 0.95 \pm 0.01 for the GCK). Compared to the previous research (i.e., Kang et al., 2012), the results
15 from the MSH were closer to the observation due to the consideration of ET from the dry canopy. One of the leading causes of the error in λET_{WC_MSH} was identified as the discrepancy between the time when the rain occurred, and the tipping bucket was tipped. The results from the further evaluation of the MSH using a closed-path EC system were similar to those using the open-path EC system (see the Appendix C). To validate only E_{WC} , cross-validation using the other models (e.g., Gash sparse analytical model, Gash et al., 1995) can be attempted (e.g., Kang et al., 2012). Overall, the results from the linear
20 regression analysis of λET_{WC_MSH} and λET_{WC_Obs} show that MSH can provide λET_{WC} reasonably well for the sites.

[Table 1 here]

3.2 Comparison between the MDS and the MSH

25 To evaluate the superiority of the MSH, we filled up the missing λET_{WC} data by using the MDS (λET_{WC_MDS}) and the MSH (λET_{WC_MSH}). The underestimation of the λET_{WC_MDS} had been shown by the comparison with the sum of energy flux components except for latent heat flux (= net radiation + sensible heat flux + storage flux) in our previous study (Kang et al. 2012). The λE_{WC_mod} displayed the mirrored patterns of the sum of the other energy budget components, while the λET_{WC_MDS} were very small (mainly due to the low radiation during the rainy days). Thus, we expected that the MDS underestimates the
30 ET since it cannot explicitly consider the key processes of wet canopy evaporation (i.e., the effects of aerodynamic conductance (g_a) change and sensible heat advection, see Kang et al., 2012 for more detailed explanation). Actually, the average annual MBEs from 2008 to 2010 were $-18 \pm 6 \text{ W m}^{-2}$ for the GDK site and $-15 \pm 5 \text{ W m}^{-2}$ for the GCK site,

respectively. It also should be noted that the λET_{WC_MSH} varied while λET_{WC_MDS} were nearly constant occasionally, because (1) the λET_{WC_Obs} rarely existed close to the missing data and (2) the MDS did not consider the effect of g_a (not shown here). Figure 3 shows the monthly ETs gap-filled by the MDS and MSH methods for the GDK and GCK sites. First, the annual ETs from the MSH method were $16 \sim 41 \text{ mm year}^{-1}$, which is significantly larger than those from the MDS method, while 5 the random uncertainties in gap-filled annual ETs were approximately 5 mm year^{-1} for the both sites (quantified according to Finkelstein and Sims, 2001, and Richardson and Hollinger, 2007). The significant difference was identified in June, July, August, and September when it was intensive rainfall. The biggest difference is shown in 2010 with more frequent and larger rainfall (for the GDK, the number of rainy days is 86, 82, and 103 days and the total amount of rainfall is 1,407, 1,323, and 1,652 mm in 2008, 2009, and 2010, respectively). Such characteristics are similar to those for the GCK). In addition to taking 10 the missing E_{WC} from the MDS into account, the other advantage of the MSH method is that the observed in ET and by eddy covariance system can be partitioned into transpiration (T) and E_{WC} without any additional measurement. However, it can be applied to a dense canopy only, where soil evaporation is negligible. Otherwise, (e.g., before leaf unfolding and after leaf fall), the T includes the error of the soil evaporation (E_S). Thus, there is more separating the E_{WC} than partitioning the ET. The annual E_{WC} ranged from 53 mm to 82 mm for the GDK and 78 mm to 112 mm for the GCK, which occupies 14 ~ 23% 15 and 14 ~ 19% of the annual ET, respectively.

For quantifying the E_S , the supplementary eddy covariance (EC) systems were operated at the floors of the GDK and GCK sites (Kang et al. 2009b). The annual understory ET ($\sim E_S$) from 1 June 2008 to 31 May 2009 was 59 mm for the GDK and 43 mm for the GCK, which occupied 16% and 8% of the annual ET, respectively. The decoupling factor (Ω , McNaughton and Jarvis, 1983) at the forest floor was ~ 0.15 for the both sites approximately, which indicates that the E_S was controlled 20 primarily by the VPD and surface conductance (g_s) rather than R_{sdn} . This factor also suggests that separating E_S from ET using the exponential radiation extinction model to estimate the R_{sdn} at the forest floor and the relationship between the estimated R_{sdn} and the ET when the canopy is inactive (Stoy et al., 2006) can be problematic for the sites. Considering that the accurate estimation of g_s is challenging, a supplementary measurement (e.g., low-level EC, lysimeter, sap-flow 25 measurement, and isotope) is a better approach for estimating E_S . Using the E_S measured by the low-level EC, the annual T can be estimated at 265 mm (70% of ET) for the GDK and 448 mm (78% of ET) for the GCK, while the E_{WC} estimated as 55 mm (15% of ET) and 82 mm (14% of ET), respectively (Fig. 3).

[Figure 3 here]

4 Applications

In this chapter, we illustrate the advantages of the proposed technique. The benefits are caused by the gap-filling and partitioning of the H_2O flux because the model-stats hybrid (MSH) method can take the E_{WC} into account properly and separate them from ET, which has not yet been previously possible. We hope the following chapters draw attention to the ET
5 partitioning.

4.1 Wavelet coherence analysis between ET and the rainfall

To evaluate the effect of new gap-filling, we conducted the wavelet coherence analysis between ET and rainfall for the GDK site (Fig. 4, see Hong et al. (2010) and Grinsted et al. (2004) for more details regarding the wavelet coherence analysis). From one- to the third month period, which was the three-month period in the monsoon season (i.e., the intensive rainy
10 period), high correlation (i.e., red color area) was observed between ET and rainfall in 2006, 2007, 2008, and 2009. In 2007, the rainfall amount was 200 mm lower than the average level during the study period. However, the rainfall duration was the longest, and the intensity was the lowest. In 2006, 2008, and 2009, the arrow on the high correlation area pointed left. It means a negative correlation between the two variables, reflecting that the decrease in T caused by the diminishment of R_{sdn} during the intensive rainy period. In contrast, the arrow pointed right in 2007, indicating a positive correlation. The
15 magnitude of enhanced E_{WC} was greater than that of decreased T at that time and frequency in 2007. Such a positive correlation between ET and rainfall with one- to three-month cycle in 2007 was not reported in the previous study of Hong et al. (2010) which showed a negative correlation in 2006, 2007 and 2008 at that time and frequency. This can be attributed to the improvement in ET data made by the new gap-filling method (i.e., recovering the missing E_{WC} in the general gap-filling method). During the monsoon season, the E_{WC} compensates (a portion of) the decreased T , and it can occasionally be
20 balanced (e.g., in 2010).

There are some circumstantial evidences which support that the proposed method is more appropriate for taking E_{WC} into account than the conventional method: (1) the ratio of the runoff and the precipitation (adapted from Choi et al. 2011) in 2007 was the lowest (0.60 in 2007, 0.69 ± 0.06 in the other years, i.e., the ratio of the ET to the precipitation can be the highest in 2007), while the R_{sdn} (main controlling factor of T) was the lowest (4.52 GJ m^{-2} in 2007, $4.77 \pm 0.08 \text{ GJ m}^{-2}$ in the other years)
25 due to the longest rainfall duration, (2) the interannual variabilities of the estimated catchment scale annual ET (i.e., precipitation – runoff) and ET from the MDS method occurred in opposite directions (similarly to T from the MSH method).

[Figure 4 here]

4.2 Water use efficiency at the ecosystem-level and the canopy-level

Water use efficiency (WUE) can be defined in various forms such as A_n/g_{st} (intrinsic WUE; A_n : net assimilation; g_{st} : stomatal conductance; $A_n=NPP$), A_n/T (instantaneous WUE), $A_n(1-\Phi_c)/[T(1+\Phi_w)]$ (integrated WUE; Φ_c : fraction of assimilated carbon lost in respiration; Φ_w : fraction of total water loss from non-photosynthetic parts of the plant or through open stomata at night), the GPP/T (canopy-level WUE), NPP/ET (stand-level WUE), and GPP/ET (ecosystem-level WUE) (Seibt et al., 2008; Ito and Inatomi, 2012; Ponton et al., 2006), because the spatiotemporal scale and measurement method are research-specific. Based on the original definition of WUE (i.e., the ratio of CO_2 flux to H_2O flux), we re-defined the annual ecosystem-level WUE (WUE_{Eco}) and the annual canopy-level WUE (WUE_{Canopy}) as $\Sigma NEP/\Sigma ET$ and $\Sigma NPP/\Sigma T$, respectively. For estimating ΣNPP and ΣT simply, we used 0.45 of the ratio of the NPP to GPP for the both sites (Waring et al., 1998), and 0.156 and 0.075 of the ratios of E_S to ET for the GDK and GCK, respectively (Kang et al., 2009b). From 2006 to 2010, WUE_{Eco} (WUE_{Canopy}) ranged from -0.16 (2.17) to 0.32 (2.59) $g\text{ C}\cdot(kg\text{ H}_2O)^{-1}$ for the GDK site and from 0.20 (1.93) to 0.38 (2.16) $g\text{ C}\cdot(kg\text{ H}_2O)^{-1}$ for the GCK site (Table 2). Considering the increasing trend of NEE and GPP for the GCK site, it can be identified that the interannual variabilities of WUE_{Eco} and WUE_{Canopy} occurred in opposite directions for the both sites. It was primarily caused by that E_{WC} were enhanced in 2007 and 2010 due to the weakest rainfall intensity and the largest rainfall amount, respectively. Overall, such partitioning of the total ET into E_{WC} , T , and E_S enables us to understand better how ET responses to environmental changes and the how water cycle is connected to the carbon cycle in a forest ecosystem.

[Table 2 here]

5 Conclusions

There is a special feature of the new technique proposed in this study for gap-filling and partitioning of H_2O eddy fluxes: two existing methods were merged into a new method. The marginal distribution sampling (MDS) method and the simplified Rutter spars model have merged into the model-stats hybrid (MSH) method. Such a strategy strengthens the strength and makes up for the weakness of the original methods. In this context, such attempt will and must continue. The MSH method can be applied to tropical forests because tropical forests also share three properties of temperate forests (i.e., extensive, dense, and tall). However, applying the methods to grasslands may need further validation.

Acknowledgments

This work was supported by the Korea Meteorological Administration Research and Development Program under Grant KMIPA 2015-2023, and by the Weather Information Service Engine (WISE) project, KMA-2012-0001-2. We thank Hyojung Kwon, Jinkyu Hong, Jaeill Yoo, Juyeol Yun, and Je-woo Hong for their helpful support in the data collection and other logistics. Wavelet tools used in this study are benefited from Grinsted et al. (2004).

References

Aboal, J. R., Jiménez, M. S., Morales, D., and Hernández, J. M.: Rainfall interception in laurel forest in the Canary Islands, *Agric. For. Meteorol.*, 97, 73-86, 1999.

Baldocchi, D. D., Hicks, B. B., and Meyers, T. P.: Measuring biosphere-atmosphere exchanges of biologically related gases with micrometeorological methods, *Ecology*, 69, 1331-1340, 1988.

5 Carlyle-Moses, D. E., and Price, A. G.: Modelling canopy interception loss from a Madrean pine-oak stand, northeastern Mexico, *Hydrol. Process.*, 21, 2572-2580, 2007.

Choi, H. T.: Effect of forest growth and thinning on the long-term water balance in a coniferous forest, *Korean J. Agric. For. Meteorol.*, 13, 157-164, 2011 (in Korean with English abstract).

10 Crockford, R. H., and Richardson, D. P.: Partitioning of rainfall into throughfall, stemflow and interception effect of forest type, ground cover and climate, *Hydrol. Process.*, 14, 2903-2920, 2000.

Daikoku, K., Hattori, S., Deguchi, A., Aoki, Y., Miyashita, M., Matsumoto, K., Akiyama, J., Iida, S., Toba, T., and Fujita, Y.: Influence of evaporation from the forest floor on evapotranspiration from the dry canopy, *Hydrol. Process.*, 22, 4083-4096, 2008.

15 Deardorff, J.W.: Efficient prediction of ground surface temperature and moisture, with inclusion of a layer of vegetation, *J. Geophys. Res.*, 83, 1889-1903, 1978.

Deguchi, A., Hattori, S., and Park, H. T.: The influence of seasonal changes in canopy structure on interception loss: Application of the revised Gash model, *J. Hydrol.*, 318, 80-102, 2006.

Dickinson, R. E.: Modelling evapotranspiration for three-dimensional global climate models, in *Climate Processes and 20 Climate Sensitivity*, *Geophys. Monogr. Set.*, vol. 29, edited by J.E. Hansen and T. Takahashi, pp. 58-72, AGU, Washington, D.C., 1984.

Dunkerley, D. L.: Evaporation of impact water droplets in interception processes: Historical precedence of the hypothesis and a brief literature overview, *J. Hydrol.*, 376, 599-604, 2009.

25 Fratini, G., Ibrom, A., Arriga, N., Burba, G., and Papale, D.: Relative humidity effects on water vapour fluxes measured with closed-path eddy-covariance systems with short sampling lines, *Agric. For. Meteorol.*, 165, 53-63, 2012.

Gash, J. H., Lloyd, C. R., and Lachaud, G.: Estimating sparse forest rainfall interception with an analytical model, *J. Hydrol.*, 170, 79-86, 1995.

Goodrich, J. P., Oechel, W. C., Gioli, B., Moreaux, V., Murphy, P. C., Burba, G., and Zona, D.: Impact of different eddy covariance sensors, site set-up, and maintenance on the annual balance of CO₂ and CH₄ in the harsh Arctic 30 environment, *Agric. For. Meteorol.*, 228, 239-251, 2016.

Grinsted, A., Moore, J. C., and Jevrejeva, S.: Application of the cross wavelet transform and wavelet coherence to geophysical time series, *Nonlinear Process Geophys.*, 11, 561-566, 2004.

Hong, J., and Kim, J.: Impact of the Asian monsoon climate on ecosystem carbon and water exchanges: a wavelet analysis and its ecosystem modeling implications, *Global Change Biol.*, 17, 1900-1916, 2011.

Hong, J., Kim, J., Lee, D., and Lim, J. H.: Estimation of the storage and advection effects on H₂O and CO₂ exchanges in a hilly KoFlux forest catchment, *Water Resour. Res.*, 44, 2008.

5 Hong, J., Kwon, H.-J., Lim, J.-H., Byun, Y.-H., Lee, J.-H., and Kim, J.: Standardization of KoFlux eddy-covariance data processing, *Korean J. Agric. For. Meteorol.*, 11, 19-26, 2009 (in Korean with English abstract).

Hong, J., Lee, D., Kim, J.: Lessons from FIFE (First ISLSCP Field Experiment) inscaling issues of surface fluxes at Gwangneung supersite. *Korean J. Agric. For. Meteorol.* 7, 4-14, 2005 (in Korean with English abstract).

Hu, Z., Yu, G., Zhou, Y., Sun, X., Li, Y., Shi, P., Wang, Y., Song, X., Zheng, Z., and Zhang, L.: Partitioning of 10 evapotranspiration and its controls in four grassland ecosystems: Application of a two-source model, *Agric. For. Meteorol.*, 149, 1410-1420, 2009.

Hwang, Y., Ryu, Y., Kimm, H., Jiang, C., Lang, M., Macfarlane, C., and Sonnentag, O.: Correction for light scattering combined with sub-pixel classification improves estimation of gap fraction from digital cover photography, *Agric. For. Meteorol.*, 222, 32-44, 2016.

15 Ibrom, A., Dellwik, E., Flyvbjerg, H., Jensen, N. O., and Pilegaard, K.: Strong low-pass filtering effects on water vapour flux measurements with closed-path eddy correlation systems, *Agric. For. Meteorol.*, 147, 140-156, 2007.

Ito, A., and Inatomi, M.: Water-use efficiency of the terrestrial biosphere: a model analysis focusing on interactions between the global carbon and water cycles, *J. Hydrometeorol.*, 13, 681-694, 2012.

Jones, H. G.: Plants and microclimate: a quantitative approach to environmental plant physiology, Cambridge university 20 press, 9-46, 2013.

Kang, M., Kim, J., Kim, H.-S., Thakuri, B. M., and Chun, J.-H.: On the nighttime correction of CO₂ flux measured by eddy covariance over temperate forests in complex terrain, *Korean Journal of Agric. For. Meteorol.*, 16, 233-245, 2014 (in Korean with English abstract).

Kang, M., Kwon, H., Cheon, J. H., and Kim, J.: On estimating wet canopy evaporation from deciduous and coniferous 25 forests in the Asian monsoon climate, *J. Hydrometeorol.*, 13, 950-965, 2012.

Kang, M., Park, S., Kwon, H., Choi, H. T., Choi, Y. J., and Kim, J.: Evapotranspiration from a deciduous forest in a complex terrain and a heterogeneous farmland under monsoon climate, *Asia-Pac. J. Atmos. Sci.*, 45, 175-191, 2009a.

Kang, M., Ruddell, B. L., Cho, C., Chun, J., and Kim, J.: Identifying CO₂ advection on a hill slope using information flow, *Agric. For. Meteorol.*, 232, 265-278, 2017.

30 Kang, M., Kwon, H., Lim, J.-H., and Kim, J.: Understory evapotranspiration measured by eddy-covariance in Gwangneung deciduous and coniferous forests, *Korean J. Agric. For. Meteorol.*, 11, 233-246, 2009b (in Korean with English abstract).

Kang, M., Thakuri, M. B., Kim, J., Chun, J., and Cho, C.: A modification of the moving point test method for nighttime eddy flux filtering on hilly and complex terrain, Abstract B41B-0404 presented at 2016 Fall Meeting, AGU, San Francisco, Calif., 2016.

5 Kim, J., Lee, D., Hong, J., Kang, S., Kim, S.-J., Moon, S.-K., Lim, J.-H., Son, Y., Lee, J., Kim, S., Woo, N., Kim, K., Lee, B., Lee, B.-L., and Kim, S.: HydroKorea and CarboKorea: cross-scale studies of ecohydrology and biogeochemistry in a heterogeneous and complex forest catchment of Korea, *Ecol. Res.*, 21, 881-889, 2006.

Kim, J., and Verma, S. B.: Components of surface energy balance in a temperate grassland ecosystem, *Bound.-Layer Meteor.*, 51, 401-417, 1990.

Kwon, H., Park, T.-Y., Hong, J., Lim, J.-H., and Kim, J.: Seasonality of Net Ecosystem Carbon Exchange in Two Major Plant 10 Functional Types in Korea, *Asia-Pac. J. Atmos. Sci.*, 45, 149-163, 2009.

Lankreijer, H., Lundberg, A., Grelle, A., Lindroth, A., and Seibert, J.: Evaporation and storage of intercepted rain analysed by comparing two models applied to a boreal forest, *Agric. For. Meteorol.*, 98-99, 595-604, 1999.

Liang, X., Lettenmaier, D. P., Wood, E. F., and Burges, S. J.: A simple hydrologically based model of land surface water and energy fluxes for general circulation models, *J. Geophys. Res. Atmos.*, 99, 14415-14428, 1994.

15 Macfarlane, C., Hoffman, M., Eamus, D., Kerp, N., Higginson, S., McMurtrie, R., and Adams, M.: Estimation of leaf area index in eucalypt forest using digital photography, *Agric. For. Meteorol.*, 143, 176-188, 2007.

Marin, C. T., Bouting, W., and Sevink, J.: Gross rainfall and its partitioning into throughfall, stemflow and evaporation of 20 intercepted water in four forest ecosystems in western Amazonia, *J. Hydrol.*, 237, 40-57, 2000.

Matsuo, T., Sasyo, Y., and Sato, Y.: Relationship between types of precipitation on the ground and surface meteorological 20 elements, *J. Meteorol. Soc. Japan, Ser. II*, 59, 462-476, 1981.

Moon, S.-K., Park, S.-H., Hong, J., and Kim, J.: Spatial characteristics of Gwangneung forest site based on high resolution satellite images and DEM, *Korean J. Agric. For. Meteorol.*, 7, 115-123, 2005 (in Korean with English abstract).

Murakami, S.: Application of three canopy interception models to a young stand of Japanese cypress and interpretation in terms of interception mechanism, *J. Hydrol.*, 342, 305-319, 2007.

25 Papale, D.: Data gap filling. In *Eddy Covariance* (pp. 159-172). Springer Netherlands, 2012.

Papale, D., Reichstein, M., Aubinet, M., Canfora, E., Bernhofer, C., Kutsch, W., Longdoz, B., Rambal, S., Valentini, R., and Vesala, T.: Towards a standardized processing of Net Ecosystem Exchange measured with eddy covariance technique: algorithms and uncertainty estimation, *Biogeosciences*, 3, 571-583, 2006.

30 Papale, D., and Valentini, R.: A new assessment of European forests carbon exchanges by eddy fluxes and artificial neural network spatialization, *Global Change Biol.*, 9, 525-535, 2003.

Perrier, A.: Etude physique de l'évapotranspiration dans les conditions naturelles. III. Evapotranspiration réelle et potentielle des couverts végétaux. In *Annales agronomiques*, 1975.

Ponton, S., Flanagan, L. B., Alstad, K. P., Johnson, B. G., Morgenstern, K., Kljun, N., Black, T. A., and Barr, A. G.: Comparison of ecosystem water-use efficiency among Douglas-fir forest, aspen forest and grassland using eddy covariance and carbon isotope techniques, *Global Change Biol.*, 12, 294-310, 2006.

Pypker, T. G., Bond, B. J., Link, T. E., Marks, D., and Unsworth, M. H.: The importance of canopy structure in controlling the interception loss of rainfall: Examples from a young and an old-growth Douglas-fir forest, *Agric. For. Meteorol.*, 130, 113-129, 2005.

Rana, G., Katerji, N., Mastrorilli, M., and El Moujabber, M.: Evapotranspiration and canopy resistance of grass in a Mediterranean region. *Theor. Appl. Climatol.*, 50, 61-71, 1994.

Reichstein, M., Falge, E., Baldocchi, D., Papale, D., Aubinet, M., Berbigier, P., Bernhofer, C., Buchmann, N., Gilmanov, T., Granier, A., Grunwald, T., Havrankova, K., Ilvesniemi, H., Janous, D., Knohl, A., Laurila, T., Lohila, A., Loustau, D., Matteucci, G., Meyers, T., Miglietta, F., Ourcival, J.-M., Pumpanen, J., Rambal, S., Rotenberg, E., Sanz, M., Tenhunen, J., Seufert, G., Vaccari, F., Vesala, T., Yakir, D., and Valentini, R.: On the separation of net ecosystem exchange into assimilation and ecosystem respiration: review and improved algorithm, *Global Change Biol.*, 11, 1424-1439, doi:10.1111/j.1365-2486.2005.001002.x, 2005.

Reichstein, M., Stoy, P. C., Desai, A. R., Lasslop, G., and Richardson, A. D.: Partitioning of net fluxes. In *Eddy Covariance* (pp. 263-289). Springer Netherlands, 2012.

Schellekens, J., Scatena, F. N., Bruijnzeel, L. A., and Wickel, A. J.: Modelling rainfall interception by a lowland tropical rain forest in northeastern Puerto Rico, *J. Hydrol.*, 225, 168-184, 1999.

Seibt, U., Rajabi, A., Griffiths, H., and Berry, J. A.: Carbon isotopes and water use efficiency: sense and sensitivity, *Oecologia*, 155, 441, 2008.

Shi, Z., Wang, Y., Xu, L., Xiong, W., Yu, P., Gao, J., and Zhang, L.: Fraction of incident rainfall within the canopy of a pure stand of *Pinus armandii* with revised Gash model in the Liupan Mountains of China, *J. Hydrol.*, 385, 44-50, 10.1016/j.jhydrol.2010.02.003, 2010.

Shuttleworth, W., Leuning, R., Black, T., Grace, J., Jarvis, P., Roberts, J., and Jones, H.: Micrometeorology of temperate and tropical forest, *Phil. Trans. R. Soc. B*, 324, 299-334, 1989.

Silva, I. C., and Okumura, T.: Rainfall partitioning in a mixed white oak forest with dwarf bamboo undergrowth, *J. Environ. Hydrol.*, 4, XIII-XIV, 1996.

Šraj, M., Brilly, M., and Mikoš, M.: Rainfall interception by two deciduous Mediterranean forests of contrasting stature in Slovenia, *Agric. For. Meteorol.*, 148, 121-134, 2008.

Stoy, P. C., Katul, G. G., Siqueira, M. B. S., Juang, J. Y., Novick, K. A., McCarthy, H. R., Oishi, A. C., Uebelherr, J. M., Kim, H. S., and Oren, R.: Separating the effects of climate and vegetation on evapotranspiration along a successional chronosequence in the southeastern US, *Global Change Biol.*, 12, 2115-2135, 10.1111/j.1365-2486.2006.01244.x, 2006.

Thom, A. S.: Momentum, Mass, and Heat Exchange of Vegetation, *Quart. J. Roy. Meteor. Soc.*, 98, 124–134, 1972.

Valente, F., David, J. S., and Gash, J. H. C.: Modelling interception loss for two sparse eucalypt and pine forests in central Portugal using reformulated Rutter and Gash analytical models, *J. Hydrol.*, 190, 141-162, 1997.

Van Dijk, A. I. J. M., and Bruijnzeel, L. A.: Modelling rainfall interception by vegetation of variable density using an adapted analytical model. Part 2. Model validation for a tropical upland mixed cropping system, *J. Hydrol.*, 247, 5 239-262, 2001.

van Gorsel, E., Delpierre, N., Leuning, R., Black, A., Munger, J. W., Wofsy, S., Aubinet, M., Feigenwinter, C., Beringer, J., and Bonal, D.: Estimating nocturnal ecosystem respiration from the vertical turbulent flux and change in storage of CO₂, *Agric. For. Meteorol.*, 149, 1919-1930, 2009.

Waring, R., Landsberg, J., and Williams, M.: Net primary production of forests: a constant fraction of gross primary 10 production?, *Tree physiol.*, 18, 129-134, 1998.

Webb, E. K., Pearman, G. I., and Leuning, R.: Correction of flux measurements for density effects due to heat and water vapour transfer, *Q. J. R. Meteorol. Soc.*, 106, 85-100, 10.1002/qj.49710644707, 1980.

Wilczak, J., Oncley, S., and Stage, S.: Sonic Anemometer Tilt Correction Algorithms, *Boundary-Layer Meteorol.*, 99, 127-150, 2001.

15 Willmott, C. J.: Some comments on the evaluation of model performance, *Bull. Amer. Meteor. Soc.*, 63, 1309-1313, 1982.

Willmott, C. J., and Matsuura, K.: Advantages of the mean absolute error (MAE) over the root mean square error (RMSE) in assessing average model performance, *Climate Res.*, 30, 79-82, 10.3354/cr030079, 2005.

Wilson, K. B., Hanson, P. J., Mulholland, P. J., Baldocchi, D. D., and Wullschleger, S. D.: A comparison of methods for determining forest evapotranspiration and its components: sap-flow, soil water budget, eddy covariance and 20 catchment water balance, *Agric. For. Meteorol.*, 106, 153-168, 2001.

Yepez, E. A., Williams, D. G., Scott, R. L., and Lin, G.: Partitioning overstory and understory evapotranspiration in a semiarid savanna woodland from the isotopic composition of water vapor, *Agric. For. Meteorol.*, 119, 53-68, 2003.

Yoo, J., Lee, D., Hong, J., and Kim, J.: Principles and Applications of Multi-Level H₂O/CO₂ Profile Measurement System, *Korean J. Agric. For. Meteorol.*, 11, 27-38, 2009 (in Korean with English abstract).

25 Yuan, R., Kang, M., Park, S., Hong, J., Lee, D., and Kim, J.: The effect of coordinate rotation on the eddy covariance flux estimation in a hilly KoFlux forest catchment, *Korean J. Agric. For. Meteorol.*, 9, 100-108, 2007.

Yuan, R., Kang, M., Park, S., Hong, J., Lee, D., and Kim, J.: Expansion of the planar-fit method to estimate flux over complex terrain, *Meteorol. Atmos. Phys.*, 110, 123-133, 2011.

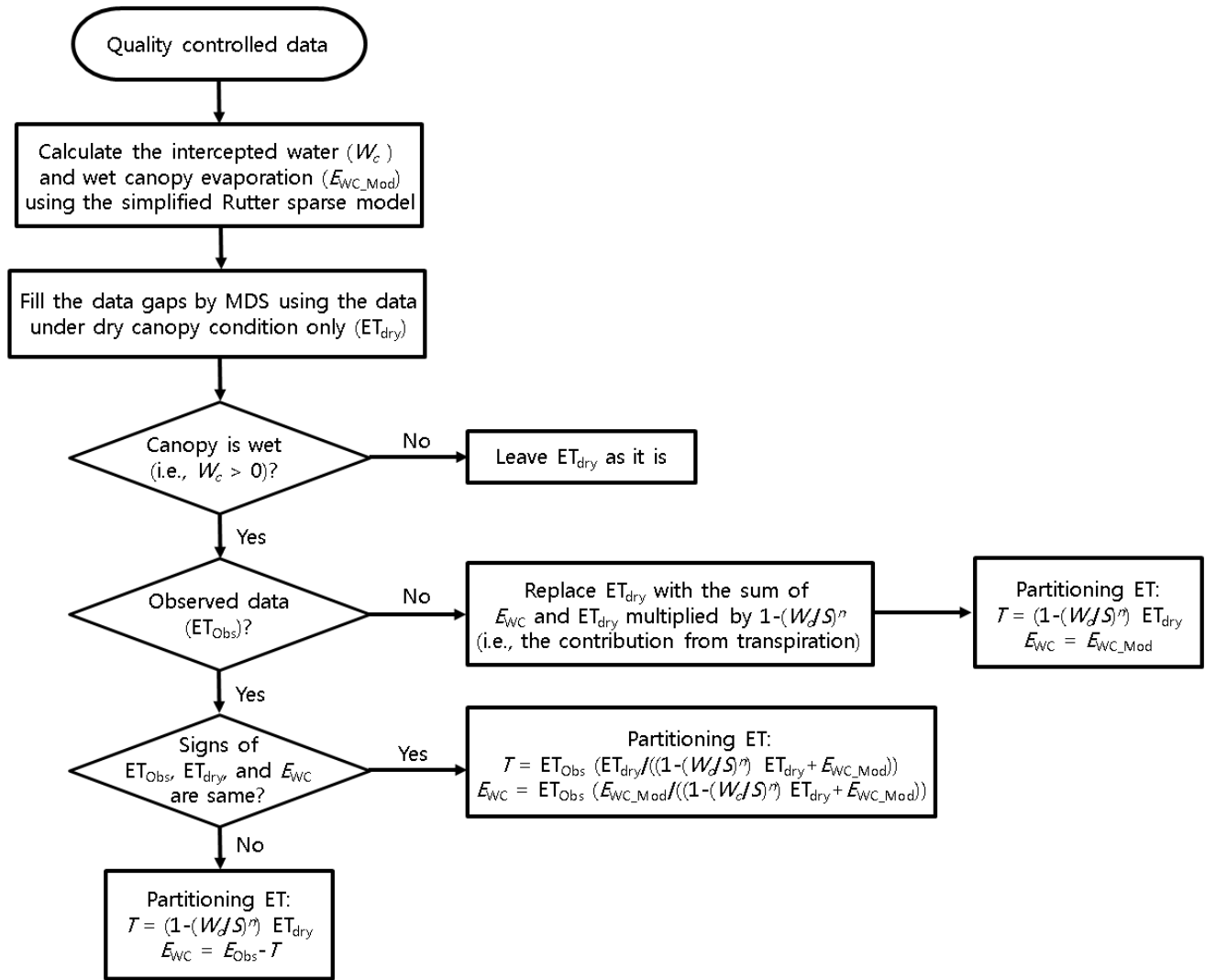


Figure 1: Flowchart of the gap-filling and partitioning technique for evapotranspiration.

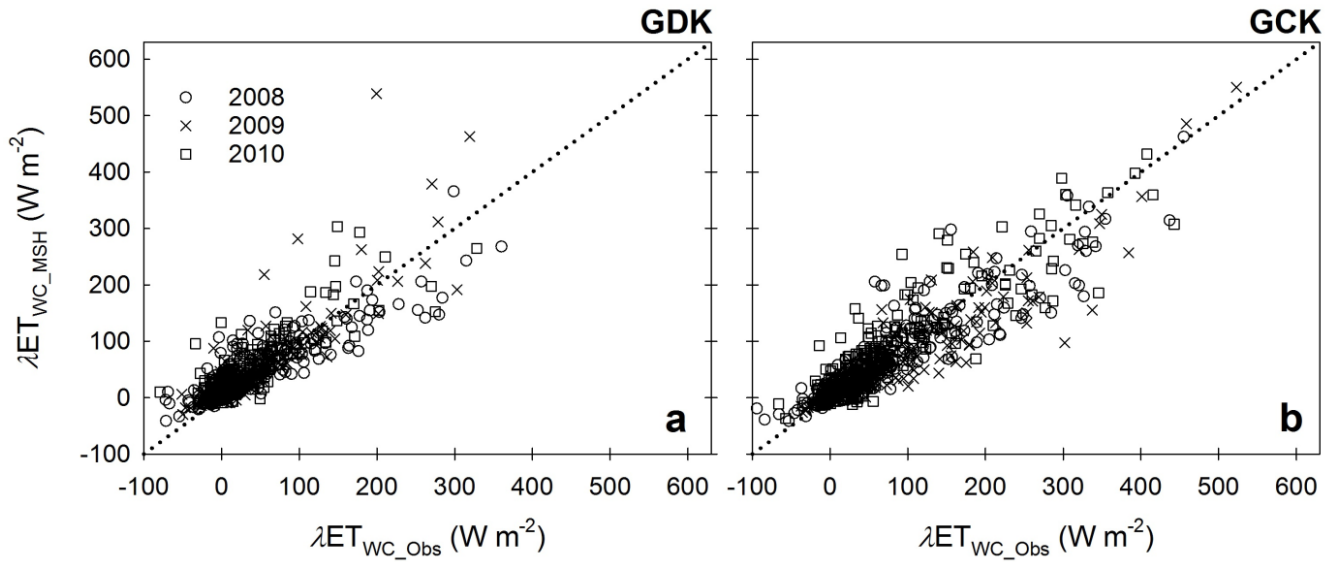


Figure 2: Comparison of the latent heat flux under (mostly) wet canopy condition (i.e., $W_c/S > 2/3$ where W_c is the intercepted canopy water and S is the canopy storage capacity) at the GDK (a) and GCK (b) sites; λET_{WC_Obs} indicates the observed latent heat flux under a wet canopy condition (λET_{WC}), while λET_{WC_MSH} indicates the estimated λET_{WC} using the model-stats hybrid method. The dotted line represents the 1:1 line.

5

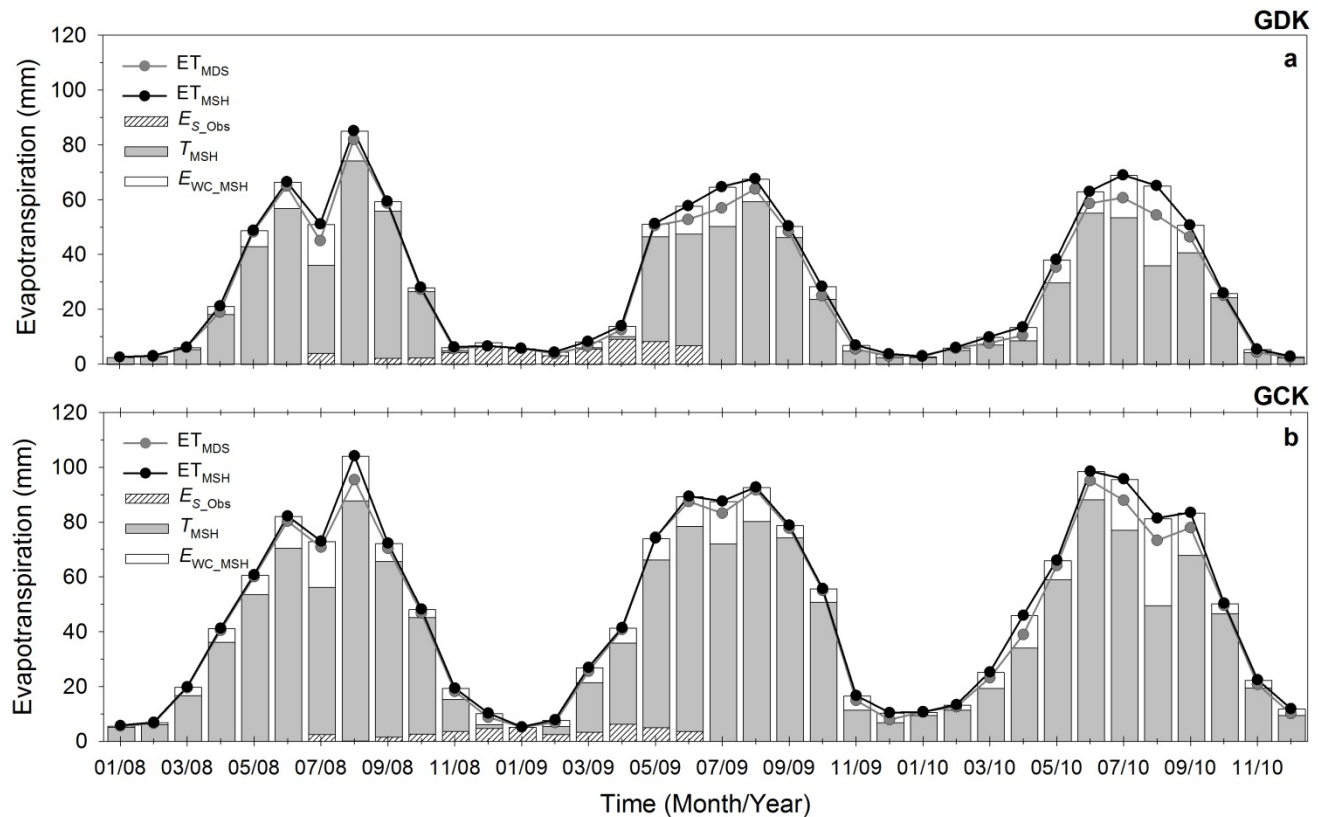
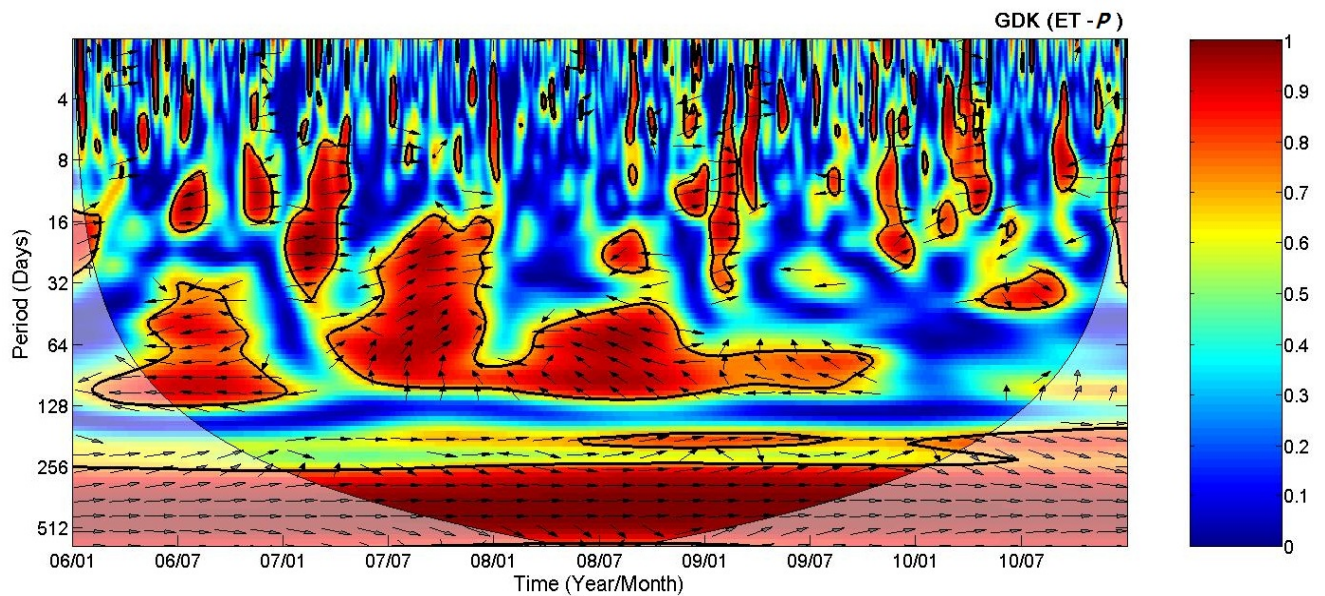


Figure 3: Seasonal variation of monthly integrated evapotranspiration (ET) with the gap-filled by the marginal distribution sampling method (ET_{MDS}); the ET gap-filled by the model-stats hybrid (MSH) method (ET_{MSH}), transpiration and wet canopy evaporation partitioned by the MSH method (T_{MSH} and E_{WC_MSH}), for the GDK (a) and GCK (b) sites. E_{S_Obs} indicates soil evaporation measured by the supplementary eddy covariance systems at the floors (adapted from Kang et al., 2009b).



5 **Figure 4:** Wavelet coherence spectrum of evapotranspiration (ET) with rainfall (P) for the GDK site. A thick solid contour is the 5% significance level against red noise as calculated from a Monte Carlo simulation. Arrows are the relative phase angle (with in-phase (positive correlation) pointing right, antiphase (negative correlation) pointing left, and P leading ET by 90° pointing straight down). The shaded area indicates the cone of influence where the edge effects might distort the results.

Table 1: Statistical parameters for the error assessment at the study sites. MBE, MAE, RMSE, and d indicate mean bias error, mean absolute error, root mean square error, and index of agreement, respectively. Slope and r^2 are from the linear regression analysis.

		No. of data	MBE	MAE	RMSE	d	Slope	r^2
		--	W m^{-2}	W m^{-2}	W m^{-2}	--	--	--
GDK	2008	333	6	20	30	0.93	0.80	0.72
	2009	222	12	21	39	0.91	1.10	0.73
	2010	215	14	23	34	0.90	1.00	0.63
GCK	2008	318	-4	23	36	0.95	0.84	0.83
	2009	246	-10	26	44	0.94	0.85	0.79
	2010	285	7	24	39	0.95	0.97	0.82

Table 2: The annual CO₂ and H₂O budget (NEE: net ecosystem exchange, GPP: gross primary production, RE: ecosystem respiration, ET: evapotranspiration, E_{WC} : wet canopy evaporation) and water use efficiency at the ecosystem-level (WUE_{Eco}) and the canopy-level (WUE_{Canopy}) for the study sites.

	NEE	GPP	RE	ET	E_{WC}	WUE _{Eco}	WUE _{Canopy}
	g C m ⁻² y ⁻¹	g C m ⁻² y ⁻¹	g C m ⁻² y ⁻¹	mm	mm	g C·(kg H ₂ O) ⁻¹	g C·(kg H ₂ O) ⁻¹
GDK	2006	-114	1,149	1,035	361	66	0.32
	2007	-14	1,183	1,169	398	116	0.03
	2008	-84	1,326	1,242	383	53	0.22
	2009	-45	1,346	1,301	360	56	0.12
	2010	58	1,242	1,300	353	82	-0.16
GCK	2007	-109	1,892	1,783	557	122	0.20
	2008	-186	1,822	1,636	544	78	0.34
	2009	-174	2,190	2,016	587	77	0.30
	2010	-233	2,140	1,907	606	112	0.38

Appendix A: Parameterizations of canopy storage

The rainfall interception is sensitive to the change of canopy storage capacity (S) and vegetation fraction (σ_f i.e., 1-gap fraction) (e.g., Shi et al., 2010). One of the characteristics common among the temperate forests considered in this study is a dense canopy. It means that the vegetation fractions in the forests are close to 1 (except before leaf unfolding and after leaf

5 fall periods). Moreover, the gap fraction can be measured using a plant canopy analyzer with relative ease. Therefore, the error of the result from the model is mostly derived from the parameterization of S (see Appendix B for more detailed information). The canopy storage capacity is affected by not only leaf area but also the other factors such as leaf shape, leaf angle, leaf/shoot clumping and hydrophobicity (water repellency) of a leaf (e.g., Crockford and Richardson, 2000). Additionally, the relationships between S and these characteristics are changeable according to meteorological conditions

10 (e.g., the wind, rainfall intensity), which make the parameterization of S difficult (e.g., Dunkerley, 2009). Therefore, we used the simple parameterization of S of VIC LSM (i.e., $S = K_L \times$ leaf (or plant) area index, where $K_L = 0.2$; Liang et al., 1994) and evaluated whether the parameterization was reasonable or not. The relationships between the leaf area index (LAI) and S in the previous studies are presented in Fig. A1, indicating that the parameterization in VIC LSM (i.e., $K_L = 0.2$) is reasonable and the K_L ranges from 0.1 to 0.3. Further studies on the parameterization of S using leaf structure (e.g., leaf

15 shape, leaf angle, leaf/shoot clumping) would be worth conducting for more accurate estimation of wet canopy evaporation.

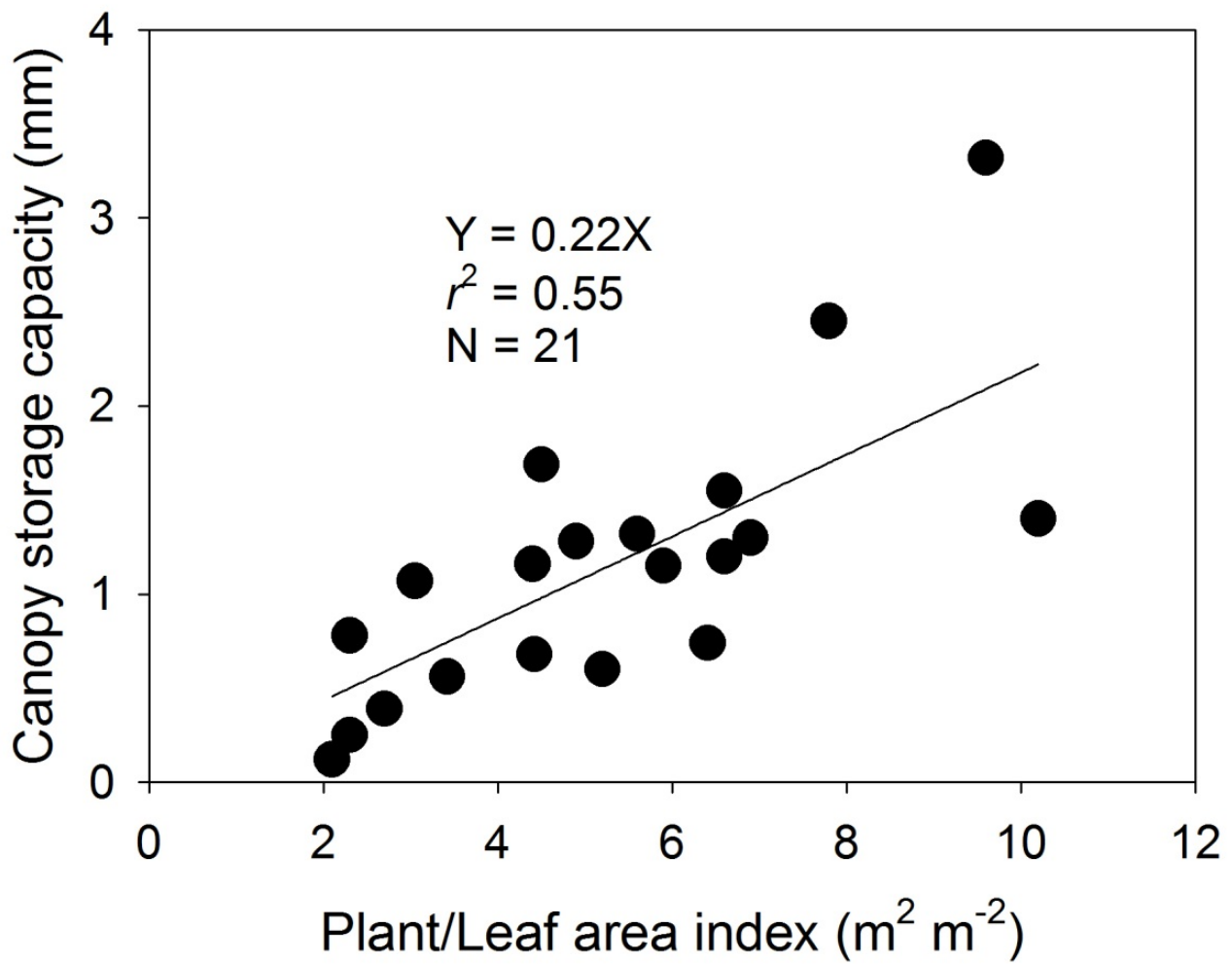


Figure A1: Relationship between canopy storage capacity and plant/leaf area index (the data obtained from Table A1).

Table A1: Review of the canopy storage capacity for wet canopy evaporation modeling in the previous studies.

Vegetation type	Species	Country	Longitude /Latitude	Canopy storage capacity (mm)	Plant/Leaf area index (m ² m ⁻²)	Density (trees ha ⁻¹)	References
Laurel forest	<i>Myrica faya</i> Ait., <i>Laurus azorica</i> (Seub.) Franco, <i>Persea indica</i> (L.) Spreng, <i>Erica arborea</i> L., <i>Ilex perado</i> ssp. <i>plathypylla</i> Webb & Amarra, <i>Ilex canariensis</i> Poivet	Spain	28°27'N, 16°24'W	2.45	7.8	1,693	Aboal et al. (1999)
Pine-oak forests	<i>Pinus pseudostrobus</i> , <i>Q.canbyi</i> , <i>Q.laeta</i>	Mexico	24°42.3'N, 99°52.2'W	0.78	2.3	819	Carlyle-Moses and Price (2007)
Mixed agricultural cropping system	<i>Manihot esculenta</i> Crantz, <i>Zeamays</i> L., <i>Oryza sativa</i> L.	Indonesia	7°03'S, 108°04'W	0.12	2.1		van Dijk and Bruijnzeel (2001)
Plantation forest of Maritime pine	<i>Pinus pinaster</i> Ait.	France	44°5'N, 0°5'W	0.25	2.3	430	Gash et al. (1995)
Norway spruce and Scots pine	<i>Picea abies</i> (L.) Karst., <i>Pinus sylvestris</i> (L.)	Sweden	60°5'N, 17°29'E	1.69	4.5		Lankreijer et al. (1999)
Secondary broad leaved deciduous forests	<i>Quercus serrara</i> , <i>Clethra barbinervis</i>	Japan	35°02'N, 137°11'E	1.07	3.05		Deguchi et al. (2006)
Mature rain forests		Colombian Amazonia		1.16	4.4		
				1.28	4.9		Marin et al. (2000)
				1.32	5.6		
				1.55	6.6		
Tabonuco type forest	<i>Dacryodes excelsa</i>	Puerto Rico	18°18N, 65°5'W	1.15	5.9		Schellekens et al. (1999)
Mixed White Oak Forest	<i>Quercus serrata</i> Thunb., <i>Sasa paniculata</i> Makino et Shibata.	Japan	35°19'N, 133°35'E	0.6	5.2		Silva and Okumura (1996)
Secondary broad-leaved deciduous forests(Summer)		Japan		0.68	4.42		Park (2000)
Secondary broad-leaved				0.39	2.7		

deciduous forests(Winter)				
Secondary broad-leaved deciduous forests (Summer)		0.74	6.41	
Secondary broad-leaved deciduous forests (Winter)		0.39	3.42	
Douglas-fir forest (Young)	45°49.1'N, 121°59.7'W	1.4	10.2	Pypker et al. (2005)
Douglas-fir forest (Old)	45°49.2'N, 121°54.1'W	3.32	9.6	
Deciduous mixed forest (South)	<i>Carpinusorientalis</i> <i>croaticus</i> , <i>Quercus</i> <i>pubescens</i>		1.2	6.6
Deciduous mixed forest (North)	<i>F. ormus</i> , <i>Q. pubescens</i>	1.3	6.9	Sraj et al., (2008)

Appendix B: Sensitivity test and parameter optimization of the wet canopy evaporation model

In the simplified Rutter sparse model (Liang et al., 1994), there are many parameters (e.g., σ_f , S , n , r_a , and r_0) for estimating the wet canopy evaporation (E_{WC}) and the intercepted canopy water (W_c). Since the model results may be sensitive to the parameters and the parameters may be site-specific, the parameter optimization using available flux data under wet canopy

5 condition should be accompanied for the generalization of the model. Considering that the gap-filling and partitioning are a kind of interpolation and extrapolation (i.e., identifying relationships between a target flux and its drivers, and interpolating and extrapolating the relationships), it is an appropriate strategy for the gap-filling and partitioning of evapotranspiration using the model.

First, we conducted a sensitivity test of the model to the parameters (i.e., k , K_L , n , and r_0) using the dataset in 2008

$$10 \quad (\text{Change in } E_{WC} \text{ } (\%)) = \frac{E_{WC_perturb} - E_{WC_default}}{E_{WC_default}} \times 100, \quad E_{WC_default}: \text{Annually integrated } E_{WC} \text{ simulated with default}$$

parameters, $E_{WC_perturb}$: Annually integrated E_{WC} simulated after a change in each parameter. Only one parameter is changed one at a time, while other parameters are held in constants, e.g., Shi et al., 2010). Before testing the sensitivity, we set the lower/upper boundaries (and default values) based on the literature reviews: $k = 0.3 \sim 1.5$ (Jones, 2013; The default values of k are 0.75 and 0.485 for the GDK and GCK, respectively. Those values were obtained from the actual measurement using a

15 plant canopy analyzer (Model LAI-2000; Li-Cor Inc.); $K_L = 0.1 \sim 0.3$ (see Appendix B; The default values of K_L is 0.2 (Dickinson, 1984).); $n = 0.5 \sim 1$ (Chen and Dudhia, 2001; Liang et al., 1994; Valente et al., 1997; The default values of n is 2/3 (Deardorff, 1978).); $r_0 = 0$ (for short vegetation) $\sim 2 \text{ s m}^{-1}$ (for tall vegetation) (Perrier, 1975; Rana et al., 1993; The default values of r_0 is 2 (Perrier, 1975).). K_L is the most influential parameters (Fig. B1), implying that we should take great care to minimize parameter estimation error for K_L .

20 Using a small number of the observed latent heat flux data under wet canopy condition (when $W_c/S > 2/3$) from 2008 to 2010, we optimized the parameters except k (because we obtained the k from the actual measurement) towards minimizing the root mean square error of the method (using the bound constrained optimization code in MATLAB[®], “fminsearchbnd.” <http://kr.mathworks.com/matlabcentral/fileexchange/8277-fminsearchbnd--fminsearchcon>). We randomly divided the available dataset into the datasets for parameter optimization and validation (i.e., validation after optimization). The ratio of

25 the optimization-validation datasets was arbitrarily set to 7:3. Table B1 shows the model parameters and the statistical parameters for the error assessment before and after the parameter optimization. After the optimization, the parameters slightly changed from the default values. However, we still used the default values conservatively since the model results from before and after the optimization were not statistically different in the error assessment.

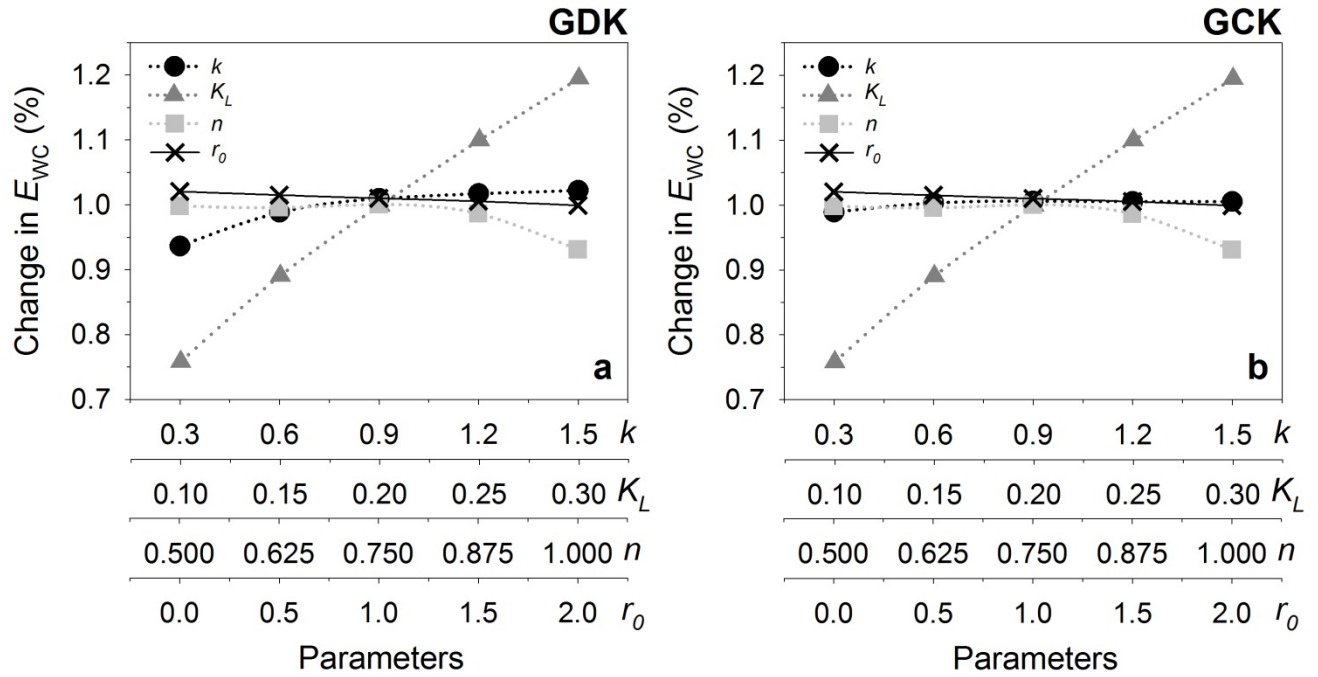


Figure B1: Sensitivity test of the wet canopy evaporation model to the parameters (i.e., k , K_L , n , and r_0).

Table B1: Statistical parameters before and after the parameter optimization for the error assessment at the study sites. MBE, MAE, RMSE, and d indicate mean bias error, mean absolute error, root mean square error, and index of agreement, respectively. Slope and r^2 are from the linear regression analysis. The default values of K_L , n , and r_0 were 0.2 (0.2), 2/3 (2/3), and 2 (2) for the GDK (GCK), respectively. After the optimization, those values changed to 0.1966 (0.2314), 0.7279 (0.6930), and 2 (2) for the GDK (GCK), respectively.

		MBE	MAE	RMSE	d	Slope	r^2
		W m ⁻²	W m ⁻²	W m ⁻²	--	--	--
GDK	Optimization dataset ($N = 538$)	before optim.	10	22	36	0.91	0.93
		after optim.	10	22	36	0.91	0.92
	Validation dataset ($N = 232$)	before optim.	10	19	29	0.93	0.96
		after optim.	10	19	29	0.93	0.96
GCK	Optimization dataset ($N = 593$)	before optim.	-2	24	41	0.95	0.89
		after optim.	-2	24	41	0.95	0.90
	Validation dataset ($N = 256$)	before optim.	-1	24	38	0.95	0.87
		after optim.	-1	24	38	0.95	0.88

Appendix C: Further evaluation of the MSH using a closed-path EC system

For further evaluation of the model-stats hybrid (MSH) method, we conducted a commercialized closed-path infrared gas analyzer with the heated tube (Model EC155, Campbell Scientific Inc., Logan, Utah, USA) from August 18, 2015 to October 25, 2015 for the GDK site. The open- and closed- path gas analyzers shared the one sonic anemometer. We applied the MSH

5 to the latent heat fluxes (λ ET) from the open-path eddy covariance (EC) system for gap-filling the λ ET under wet canopy condition, and the frequency response correction (Fratini et al., 2012) to the λ ET from the closed-path EC system for correcting the tube attenuation effect especially under high relative humidity (RH) condition. Then, we compared the λ ET (mostly) wet canopy conditions (λ ET_{WC}, i.e., λ ET when $W_c/S > 2/3$) from the MSH (λ ET_{WC_MSH_OP}) against the observed λ ET_{WC} from the closed-path EC system (λ ET_{WC_Obs_CP}) similar to the Chapter 3.1 (Fig. C1).

10 Before the comparison, it should be noted that the data retrieval rate under wet canopy condition of the closed-path EC system was 50% higher than that of the open-path EC system, however, there were still missing data for the considerable period despite the closed-path gas analyzer was conducted. The missing was mainly caused by the malfunction of the sonic anemometer and the unsatisfactory conditions for EC measurement (e.g., nonstationary and unfavorable turbulent developed conditions). The results of the error assessment (i.e., 10 W m⁻² of MBE, 19 W m⁻² of MAE, 29 W m⁻² of RMSE, 0.90 of d ,

15 1.04 of Slope, 0.68 of r^2) were within the ranges of those from the comparison between the λ ET_{WC_MSH_OP} and the λ ET_{WC_Obs} in the Chapter 3.1 (i.e., the case of the open-path EC system). Overall, such results imply the robustness of the MSH method as well as the necessity of appropriate λ ET_{WC} gap-filling method (e.g., MSH) in the case of the measurement using a closed-path EC system, like the case of an open-path EC system.

GDK

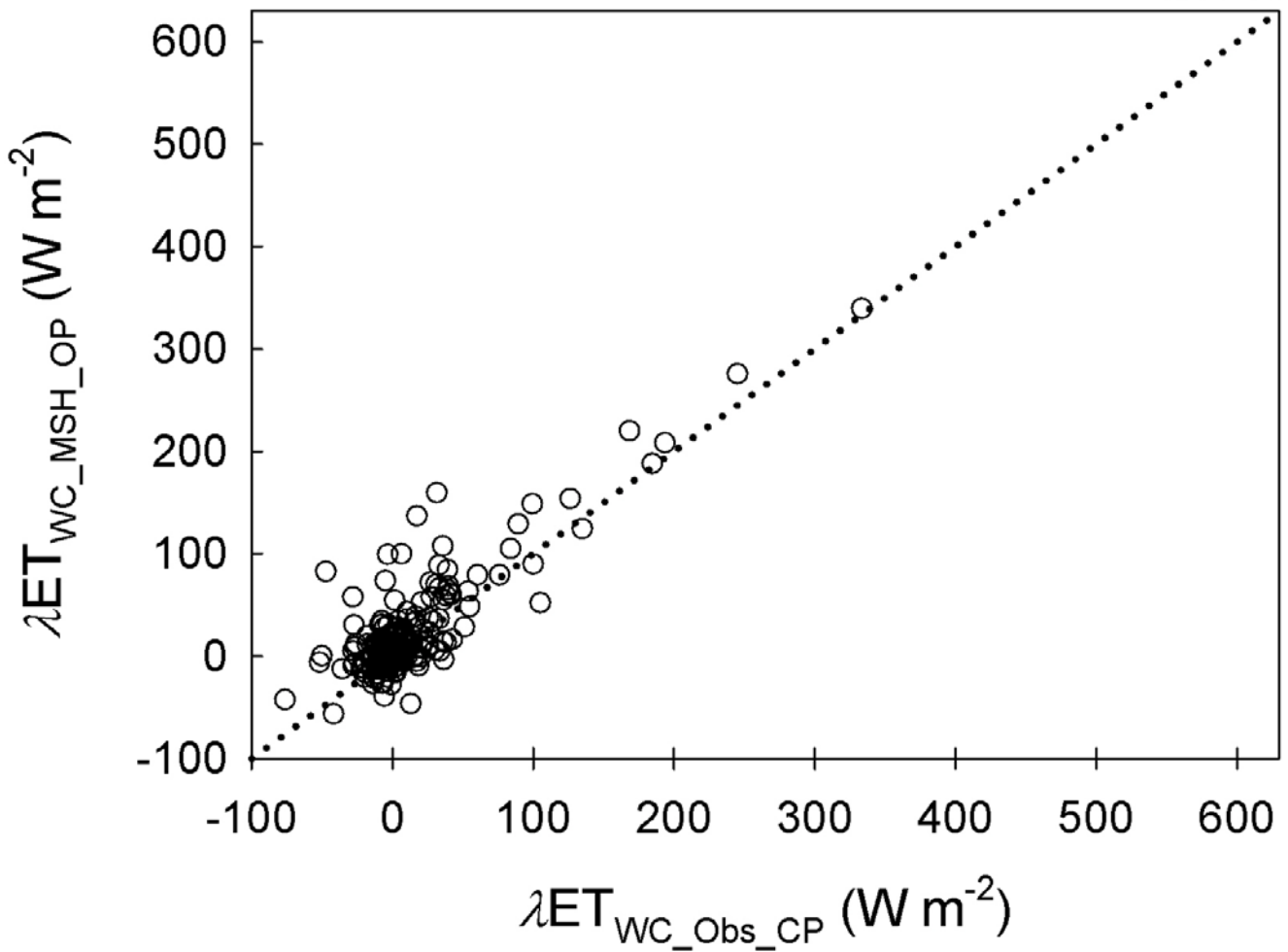


Figure C1: Comparison of the latent heat flux under (mostly) wet canopy condition (i.e., $W_c/S > 2/3$ where W_c is the intercepted canopy water and S is the canopy storage capacity) at the GDK site: $\lambda ET_{WC_Obs_CP}$ indicates the observed latent heat flux under a wet canopy condition (λET_{WC}) from a closed-path eddy covariance (EC) system, while $\lambda ET_{WC_MSH_OP}$ indicates the estimated λET_{WC} from an open-path EC system using the model-stats hybrid method. The dotted line represents the 1:1 line.

5

Appendix D: Error assessment

In order to evaluate the latent heat flux under wet canopy condition obtained from the model-stats hybrid method, we compared them against the observed data using four statistical measures, following Willmott and Matsuura (2005). Mean bias error (MBE) is the average of the residuals. Mean absolute error (MAE) is the average of the absolute values of the residuals. A large deviation from zero implies that the estimation generally overestimates or underestimates compared to the observed values. We also considered root mean squared error (RMSE) which is often reported with MAE because RMSE is more sensitive to large errors than MAE.

$$MBE = \sum \frac{Y_{\text{est}} - Y_{\text{obs}}}{n} \quad (D1)$$

$$MAE = \sum \frac{|Y_{\text{est}} - Y_{\text{obs}}|}{n} \quad (D2)$$

$$RMSE = \sqrt{\sum \frac{(Y_{\text{est}} - Y_{\text{obs}})^2}{n}} \quad (D3)$$

MBE, MAE, and RMSE give estimates of the average error, but none of them provides information about the relative size of the average difference. Thus, we further considered an additional index of agreements (d), following Willmott (1982):

$$d = 1 - \left[\frac{\sum (Y_{\text{est}} - Y_{\text{obs}})^2}{\sum (|Y_{\text{est}}' - Y_{\text{obs}}'|^2)} \right] \quad (D4)$$

where $Y_{\text{est}}' = Y_{\text{est}} - \overline{Y_{\text{obs}}}$ and $Y_{\text{obs}}' = Y_{\text{obs}} - \overline{Y_{\text{obs}}}$ (where overbar is an averaging operator). It ranges from 0 to 1, where 0 is for complete disagreement and 1 for complete agreement between the observation and the estimates. It is both a relative and bounded measure that can be widely applied in order to make cross-comparison between models.